Improvement of the GEOS-5 AGCM upon Updating the Air-Sea Roughness Parameterization

C. I. Garfinkel[1], A. Molod[2,4], L. D. Oman[3], I.-S. Song[5]

C. I. Garfinkel, Department of Earth and Planetary Science, Johns Hopkins University, Baltimore, MD 21209. (cig4@jhu.edu)

A. Molod, Global Modeling and Assimilation Office, Code 610.0, NASA/Goddard Space Flight Center, Greenbelt, MD 20771.

L. D. Oman, Atmospheric Chemistry and Dynamics Branch, Code 613.3, NASA/Goddard Space Flight Center, Greenbelt, MD 20771.

I.-S. Song, Next Generation Model Development Project, Seoul, Korea.

[1]Department of Earth and Planetary

The impact of an air-sea roughness parameterization over the ocean that more closely matches recent observations of air-sea exchange is examined in the NASA Goddard Earth Observing System, version 5 (GEOS-5) atmospheric general circulation model. Surface wind biases in the GEOS-5 AGCM are decreased by up to 1.2m/s. The new parameterization also has implications aloft as improvements extend into the stratosphere. Many other GCMs (both for operational weather forecasting and climate) use a similar class of parameterization for their air-sea roughness scheme. We therefore expect that results from GEOS-5 are relevant to other models as well.

Science, Johns Hopkins University,
Baltimore, MD.

[2]Global Modeling and Assimilation Office,
NASA/GSFC, Greenbelt, MD.

[3]Atmospheric Chemistry and Dynamics
Branch, NASA/GSFC, Greenbelt, MD.

[4]Earth System Science Interdisciplinary
Center, Univ. of MD College Park, College
Park, MD.

[5]Next Generation Model Development
Project, Seoul, Korea.

1. Introduction

The interaction between the ocean surface and the lowest levels of the atmosphere is a crucial component of any atmospheric GCM. The exchange of momentum, moisture, and sensible heat between the ocean and atmosphere occurs on spatial and temporal scales far finer than any GCM can directly simulate. Many models therefore rely on Monin-Obhukov Similarity Theory (MOST) to specify air-sea exchange as a function of bulk winds, temperature, and humidity. Early attempts at quantifying the exchange coefficients underlying MOST were conducted under conditions far removed from that actually experienced in the ocean (e.g. Charnock [1955]; Large and Pond [1981]). Nevertheless, generations of atmospheric models have relied on these earlier measurements for tuning their air-sea roughness scheme. For example, GEOS-5 currently implements Large and Pond [1981] for moderate and strong winds and Kondo [1975] for weak winds [Helfand and Schubert, 1995]. See Table 1 for a description of the schemes in a range of models.

More recent in-situ observations have improved our understanding of air-sea exchange over deep ocean waters, especially over high wind regions like the Southern Ocean. In particular, recent field campaigns have measured turbulent exchange over the Southern Ocean, over the Gulf Stream, and over the North Atlantic in high wind speeds (e.g. Edson [2008], Edson, in preparation for Journal of Physical Oceanography, Yelland et al. [1998], Edson et al. [2007], and Banner et al. [1999]). These field campaigns have found that the Charnok parameter appears to increase with wind speed beyond 10m/s, so that a parameterization based on Charnock [1955] or Large and Pond [1981] underestimates the drag on surface winds (section 3c of Fairall et al. [2003]). Recent observations of air-sea

exchange imply that the current air-sea roughness scheme in GEOS-5 produces too little drag on surface winds in the range of wind speeds common in the Southern Ocean.

Accurate climatologies of surface winds over ocean regions were not available when the current Large and Pond [1981]-based parameterization in the GEOS-5 model was created, but satellite-based climatologies of surface winds are now available (e.g. Chou et al. [2003]). These satellite based climatologies suggest that surface winds in the GEOS-5 model are too strong over the Southern Ocean and off the coast of Asia in the North Pacific (Figure 1a-c). As surface winds over the Southern Ocean drive present and future oceanic uptake of CO_2 [Downes et al., 2011; Matebr and Hirst, 1999], it is important to accurately simulate surface climate in this region. The GEOS-5 model is not alone in its poor representation of Southern Ocean surface wind; Barnes and Hartmann [2010] find that the latitude of the Southern Hemisphere jet maxima varies by over 5° in the Coupled Model Intercomparison Project (CMIP3) ensemble, and that such a bias has implications for the response of a GCM to doubled CO_2. Regional models also have difficulty capturing mesoscale turbulent surface fluxes [Renfrew et al., 2009].

This paper discusses efforts to reduce this bias in GEOS-5 by updating the air-sea roughness parameterization from Helfand and Schubert [1995]. Section 2 describes changes made to the model and Section 3 presents results. As other atmospheric GCMs base their air-sea roughness parameterization for momentum exchange on similarly old data, we expect that the reduction in model bias shown here might be common to other GCMs as well.

2. Change to Scheme

We first describe the air-sea roughness scheme in GEOS-5 before discussing the changes made to increase the surface friction. GEOS-5 contains 72 vertical levels, with approximately 8 in the boundary layer [et al., 2008]. Like many atmospheric GCMs, GEOS-5 uses MOST to describe momentum, heat, and moisture flux coefficients in terms of bulk quantities (e.g. zonal wind, specific humidity, and temperature) in the model. The wind stress vector at the surface can be expressed as

$$[\tau_x, \tau_y] = \rho_a v_s C_D \Delta[u, v]; |\tau| = \rho_a u*^2, \tag{1}$$

where ρ_a is the air density, C_D the transfer coefficient for momentum, v_s the difference between the ocean and atmosphere surface wind speed, $\Delta[u, v]$ is the difference between the ocean and atmosphere surface wind vector, and u* the friction velocity. MOST computes u* (and C_D) as a function of bulk parameters via the following equations:

$$\begin{aligned} C_D &= \kappa^2 \left[\Psi_{MO}(\zeta z_0)\right]^{-2}, \\ u* &= C_D^{1/2} v \\ z_0 &= \tfrac{A_1}{u*} + A_2 + A_3 u* + A_4 u*^2 + A_5 u*^3 \end{aligned} \tag{2}$$

where z_0 is the roughness length, κ is the Von-Karman constant, A_1 through A_5 are tunable parameters used to match the air-sea roughness scheme to observations, and $\Psi_{MO}(\zeta z_0)$ is controlled by stability of the air column above. After an initial guess is made at C_D (in practice C_D assuming neutral stability), Equation 2 is solved iteratively until a new value for C_D has been reached consistent with the actual stability.

Previously, the A_1 through A_5 coefficients were chosen to interpolate between the reciprocal relation of Kondo [1975] for weak winds and the piecewise linear relation of Large and Pond [1981] for moderate to large winds. The key change described by this paper is that the values for the A_1 through A_5 coefficients are changed so that the roughness

length is increased for a given friction velocity. Neither the formulation for $\Psi_{MO}(\zeta z_0)$ nor the coefficients at low wind speeds is changed. For very strong winds (e.g. hurricanes), roughness length no longer increases with wind speed [Molod and Partyka, 2011]. See Table 1 for the coefficients used. Runs with the old polynomial for z_0 are referred to as CONTROL, and runs with the new polynomial for z_0 are referred to as NEW.

Figure 2a shows C_{DN10m} as a function of 10m wind speed for the old and new coefficients and in observations. The drag coefficient has been increased beyond the average suggested by the most recent observations but within the uncertainty. We chose the highest drag coefficient justified by the observations to achieve the maximum impact on the GEOS-5 wind bias. Any further increase would distance us from the range of observational uncertainty. Note that the drag coefficient in Community Atmosphere Model (CAM/CCSM) (dashed red line) appears to be too small. CAM has not upgraded its scheme since version 2.0 (Kiehl et al. [1998] versus section 4.11.2 of Neale and et al. [2010]). Figure 2b compares modeled output roughness length and friction velocity for the NEW and CONTROL runs. As expected, surface roughness dramatically increases with the new coefficients. Figure 2b also includes curves of $z_0 = \alpha_{Charnok} u*^2/g$ [Charnock, 1955] but with different values of the Charnok parameter $\alpha_{Charnok}$. Older measurements suggest values of $\alpha_{Charnok}$ ~0.011 to $\alpha_{Charnok}$ ~0.018 (see Section 3c of Fairall et al. [2003]). Newer observations (Edson [2008] and Edson, manuscript in preparation for Journal of Physical Oceanography) would imply a higher $\alpha_{Charnok}$.

This change has been implemented in GEOS-5. Several GEOS-5 atmosphere-only simulations with the old and new coefficients were performed to examine the impact of the increased drag:

1. 2x2.5 degree 30 year runs with interactive stratospheric chemistry,

2. 2x2.5 degree 12 year run without interactive stratospheric chemistry,

3. 1x1.25 degree 25 year run without interactive stratospheric chemistry,

4. a series of 1/4 degree 5-day forecasts.

All simulations showed similar impact of the new roughness parameterization, and we will focus here on results from the 30 year run with stratospheric chemistry. CONTROL and NEW differ only in the air-sea roughness scheme; all other models settings are fixed. A Student-T two-tailed test is used to assess statistical significance. Each year is taken as one degree of freedom. Surface winds and surface stress from Version 2 of the Goddard Satellite-Based Surface Turbulent Fluxes (GSSTF) Data [Chou et al., 2003] are used to validate the model. We now address the impact of this change in the air-sea roughness parameterization on bulk quantities in the model.

3. Results

We now discuss how the change in friction influences the momentum budget in the model. The exchange coefficient for momentum increases over most oceanic regions, with the strongest increase over the Southern Ocean (Figure 3b). Biases in surface wind are reduced across the ocean regions in response to the altered surface roughness coefficients (Figure 1c-d). Winds over the Southern Ocean decrease by over 1m/s, but winds are

reduced over most ocean covered regions. Surface sea level pressure biases are also reduced (not shown), consistent with the wind speed improvement.

Figure 3c-f shows zonal surface stress on the ocean. Changes in surface stress are smaller than changes in either C_D or wind speed, as might be expected from Equation 1. Namely, the decrease in wind speed and increase in C_D largely balance each other, so that their product is nearly constant. Nevertheless, the changes are significant in the Southern Hemisphere, whereby surface stress on the Southern Ocean is increased while surface stress further equatorward is decreased. The change is particularly strong in the Indian Ocean/Australia region. Biases in the control run are partially ameliorated. Runs in which the atmosphere is coupled to a full ocean are planned in order to understand the potential impact on the ocean circulation.

These changes in surface stress imply anomalous eddy momentum flux convergence aloft, as vertically averaged $\frac{\partial \overline{u'v'}}{\partial y}$ must balance surface friction for a steady state surface jet (Held [1975] and section 12.1 of Vallis [2006]). Figure 4 shows that poleward momentum flux is increased throughout the upper troposphere, as implied by the dipole of surface stress. Eddies are fluxing more momentum poleward in order to counteract the weakening of the surface jet. Associated with this change in momentum flux are statistically significant improvements in extratropical forecasting skill (not shown).

4. Conclusions

The old air-sea roughness scheme in GEOS-5 is based on 30-year old observational data, but newer data suggests seas are rougher. Associated with the old parameterization are overly strong surface winds. By incorporating more recent observations of air-sea

exchange into the model's air-sea roughness scheme, we have improved the surface climate in the GEOS-5 AGCM. Preliminary results indicate that the improvement is present at resolutions up to 1/4 degree.

Modifying the air-sea roughness parameterization leads to statistically significant changes in cloud distribution, heat flux, stratospheric ozone, and planetary wave driving of the stratosphere. Presentation of these changes, a discussion of the surface moisture and sensible heat budgets, and further diagnostics on the tropospheric momentum budget, will be reported in detail in a future paper. The microphysics scheme in all runs considered does not include interactive aerosals; preliminary results indicate that including interactive aerosals along with this change in surface roughness leads to large changes in sea salt aerosal concentration and subsequent cloud formation.

Other atmospheric GCMs appear to use a similar scheme to parametrize the exchange of momentum, heat, and moisture with the ocean. We expect that biases in these other models might be reduced if these models were retuned to more closely match available observations.

Acknowledgments. This work was supported by the NASA grant number NNX06AE70G. The authors thank J. Edson for making available data from Edson [2008] and his manuscript in preparation, Larry Takacs for performing the model simulation in forecast mode, and Andrew Eichmann for performing the 1 degree model simulations.

References

M. L. Banner, W. Chen, E. J. Walsh, J. B. Jensen, S. Lee, and C. Fandry. The Southern Ocean Waves Experiment. Part I: Overview and Mean Results. *Journal of Physical Oceanography*, 29:2130–2145, September 1999. doi: 10.1175/1520-0485(1999)029⟨2130:TSOWEP⟩2.0.CO;2.

E.A. Barnes and D.L. Hartmann. Testing a theory for the effect of latitude on the persistence of eddy-driven jets using cmip3 simulations. *Geophys. Res. Lett.*, 37, 2010. doi: 10.1029/2010GL044144.

A. C. M. Beljaars. The parametrization of surface fluxes in large-scale models under free convection. *Quarterly Journal of the Royal Meteorological Society*, 121:255–270, January 1995. doi: 10.1002/qj.49712152203.

H. Charnock. Wind stress on a water surface. *Quarterly Journal of the Royal Meteorological Society*, 81:639–640, October 1955. doi: 10.1002/qj.49708135027.

S.-H. Chou, E. Nelkin, J. Ardizzone, R. M. Atlas, and C.-L. Shie. Surface Turbulent Heat and Momentum Fluxes over Global Oceans Based on the Goddard Satellite Retrievals, Version 2 (GSSTF2). *Journal of Climate*, 16:3256–3273, October 2003. doi: 10.1175/1520-0442(2003)016⟨3256:STHAMF⟩2.0.CO;2.

S. M. Downes, A. S. Budnick, J. L. Sarmiento, and R. Farneti. Impacts of wind stress on ACC fronts and subduction. *Geophys. Res. Lett.*, 2011. doi: 10.1029/2011GL047668.

J. Edson, T. Crawford, J. Crescenti, T. Farrar, N. Frew, G. Gerbi, C. Helmis, T. Hristov, D. Khelif, A. Jessup, H. Jonsson, M. Li, L. Mahrt, W. McGillis, A. Plueddemann, L. Shen, E. Skyllingstad, T. Stanton, P. Sullivan, J. Sun, J. Trowbridge, D. Vickers,

S. Wang, Q. Wang, R. Weller, J. Wilkin, A. J. Williams, D. K. P. Yue, and C. Zappa. The Coupled Boundary Layers and Air Sea Transfer Experiment in Low Winds. *Bulletin of the American Meteorological Society*, 88, 2007. doi: 10.1175/BAMS-88-3-341.

J. B. Edson. Review of Air-Sea Transfer Processes. *ECMWF Workshop on Ocean-Atmosphere Interactions, 10-12 November 2008*, 2008.

M.M. Rienecker et al. The GEOS-5 Data Assimilation System - Documentation of Versions 5.0.1, 5.1.0, and 5.2.0. *Technical Report Series on Global Modeling and Data Assimilation*, 27, 2008. URL `http://gmao.gsfc.nasa.gov/pubs/docs/Rienecker369.pdf`.

C. W. Fairall, E. F. Bradley, J. E. Hare, A. A. Grachev, and J. B. Edson. Bulk Parameterization of Air Sea Fluxes: Updates and Verification for the COARE Algorithm. *Journal of Climate*, 16:571–591, February 2003. doi: 10.1175/1520-0442(2003)016⟨0571:BPOASF⟩2.0.CO;2.

European Centre for Medium-Range Weather Forecasts. IFS DOCUMENTATION - Cy36r1 Operational implementation 26 January 2010, PART IV: PHYSICAL PROCESSES. *ECMWF TECHNICAL NOTE*, Cy36r1, 2010. doi: http://www.ecmwf.int/research/ifsdocs/CY36r1/PHYSICS/IFSPart4.pdf.

I. M. Held. Momentum Transport by Quasi-Geostrophic Eddies. *Journal of Atmospheric Sciences*, 32:1494–1496, July 1975. doi: 10.1175/1520-0469(1975)032⟨1494:MTBQGE⟩2.0.CO;2.

H. M. Helfand and S. D. Schubert. Climatology of the Simulated Great Plains Low-Level Jet and Its Contribution to the Continental Moisture Budget of the United States. *Journal of Climate*, 8:784–806, April 1995. doi: 10.1175/1520-0442(1995)008⟨0784:

COTSGP⟩2.0.CO;2.

J. T. Kiehl, J. J. Hack, G. B. Bonan, B. A. Boville, D. L. Williamson, and P. J. Rasch. The National Center for Atmospheric Research Community Climate Model: CCM3*. *Journal of Climate*, 11:1131–1150, June 1998. doi: 10.1175/1520-0442(1998)011⟨1131:TNCFAR⟩2.0.CO;2.

J. Kondo. Air-sea bulk transfer coefficients in diabatic conditions. *Bound. Layer Meteorol.*, 9:91–112, 1975.

W. G. Large and S. Pond. Open Ocean Momentum Flux Measurements in Moderate to Strong Winds. *Journal of Physical Oceanography*, 11:324–336, March 1981. doi: 10.1175/1520-0485(1981)011⟨0324:OOMFMI⟩2.0.CO;2.

W. G. Large, J. C. McWilliams, and S. C. Doney. Oceanic vertical mixing: a review and a model with a nonlocal boundary layer parameterization. *Reviews of Geophysics*, 32: 363–404, 1994. doi: 10.1029/94RG01872.

R. J. Matebr and A. C. Hirst. Climate change feedback on the future oceanic CO2 uptake. *Tellus Series B Chemical and Physical Meteorology B*, 51:722–+, July 1999. doi: 10.1034/j.1600-0889.1999.t01-1-00012.x.

GFDL model development team. The new gfdl global atmosphere and land model am2lm2: Evaluation with prescribed sst simulations. *Journal of Climate*, 17, 2004. doi: 10.1175/JCLI-3223.1. URL `http://journals.ametsoc.org/doi/abs/10.1175/JCLI-3223.1`.

Andrea Molod and Gary Partyka. The Impact on GEOS-5 Hurricane Forecasts of Limiting Ocean Roughness. *Geophys. Res. Lett.*, in prep., 2011.

L. Neale and et al. Description of the NCAR Community Atmosphere Model (CAM 5.0). *NCAR TECHNICAL NOTE*, 2010. URL `http://www.cesm.ucar.edu/models/cesm1.0/cam/docs/description/cam5_desc.pdf`.

I. A. Renfrew, G. N. Petersen, D. A. J. Sproson, G. W. K. Moore, H. Adiwidjaja, S. Zhang, and R. North. A comparison of aircraft-based surface-layer observations over Denmark Strait and the Irminger Sea with meteorological analyses and QuikSCAT winds. *Quart. J. Roy. Meteorol. Soc.*, 135, 2009. doi: 10.1002/qj.444.

William C. Skamarock, Joseph B. Klemp, Jimy Dudhia, David O. Gill, Dale M. Barker, Michael G. Duda, Xiang-Yu Huang, Wei Wang, and Jordan G. Powers. A Description of the Advanced Research WRF Version 3. *NCAR TECHNICAL NOTE*, 475, 2008. URL `http://www.mmm.ucar.edu/wrf/users/docs/arw_v3.pdf`.

G. K. Vallis. *Atmospheric and Oceanic Fluid Dynamics: Fundamentals and Large-Scale Circulation*. Cambridge University Press, 2006.

M. J. Yelland, B. I. Moat, P. K. Taylor, R. W. Pascal, J. Hutchings, and V. C. Cornell. Wind Stress Measurements from the Open Ocean Corrected for Airflow Distortion by the Ship. *Journal of Physical Oceanography*, 28:1511–1526, July 1998. doi: 10.1175/1520-0485(1998)028⟨1511:WSMFTO⟩2.0.CO;2.

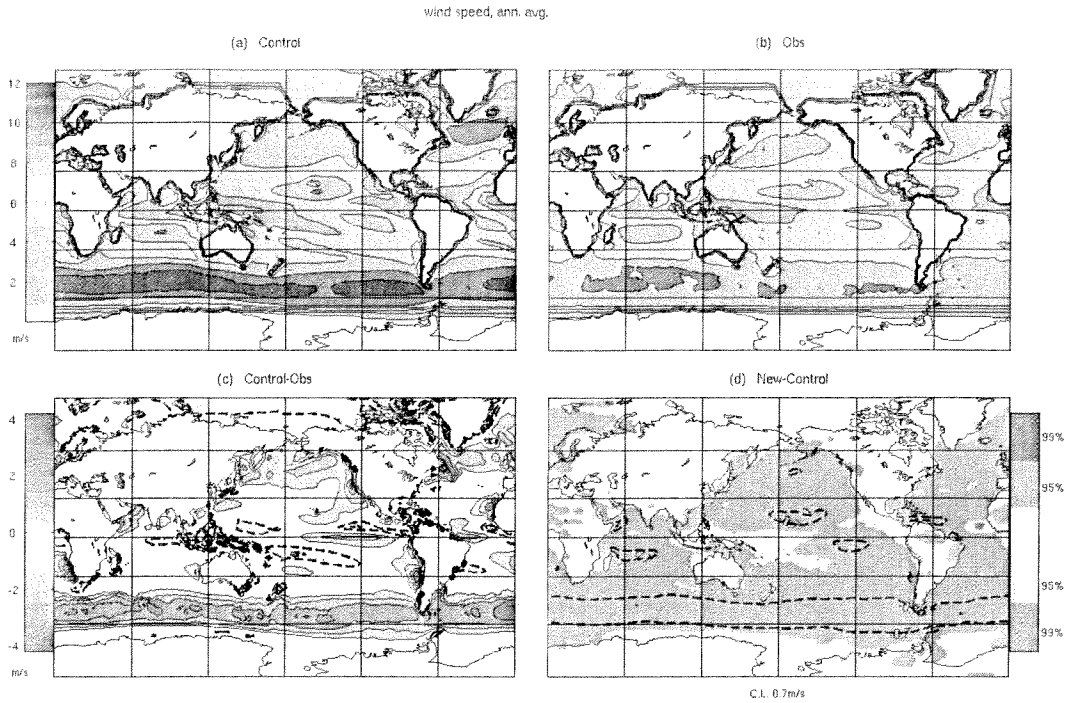

Figure 1. (a) surface wind speed in the control run, (b) surface wind speed in observations, (c) control minus the observations, and (d) the new run minus the control. For (a) and (b), the contour interval is 2m/s and the color scale is on the top left. For (c) and (d), the contour interval is 0.7 m/s. For (c), the color scale is on the left. For (d), regions with anomalies whose statistical significance exceeds 95% are in color. The zero contour is omitted and negative contours are dashed.

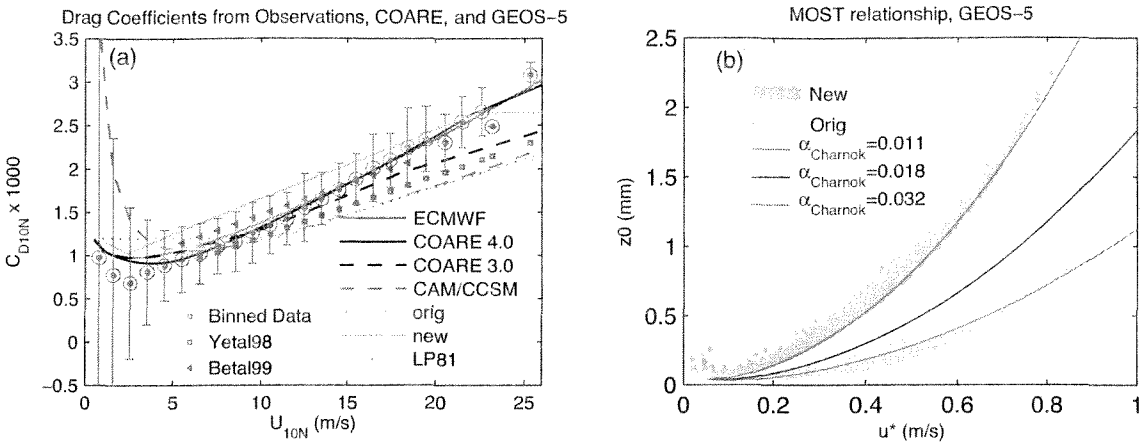

Figure 2. (a) Neutral drag coefficient for momentum exchange at the ocean surface (C_{Dn10m}) as a function of wind speed at 10m in observations [Banner et al., 1999; Yelland et al., 1998] and in models. COARE3.0, COARE4.0, ECMWF wave model (i.e. not the uncoupled atmospheric model as in Table 1), and binned data are based on Edson [2008] and Edson, personal communication. Error bars for binned data denote 1 standard deviation. Model results are from CAM2.0-CAM5 [Kiehl et al., 1998], and the original and new curves from GEOS-5. (b) Relationship between friction velocity (u*) and roughness length(z_0) over all ocean gridpoints averaged over one day of GEOS-5 model output. Isolines of $z_0 = \alpha_{Charnok} u*^2 / g$ [Charnock, 1955] but with different values of the Charnok parameter $\alpha_{Charnok}$ are included for comparison.

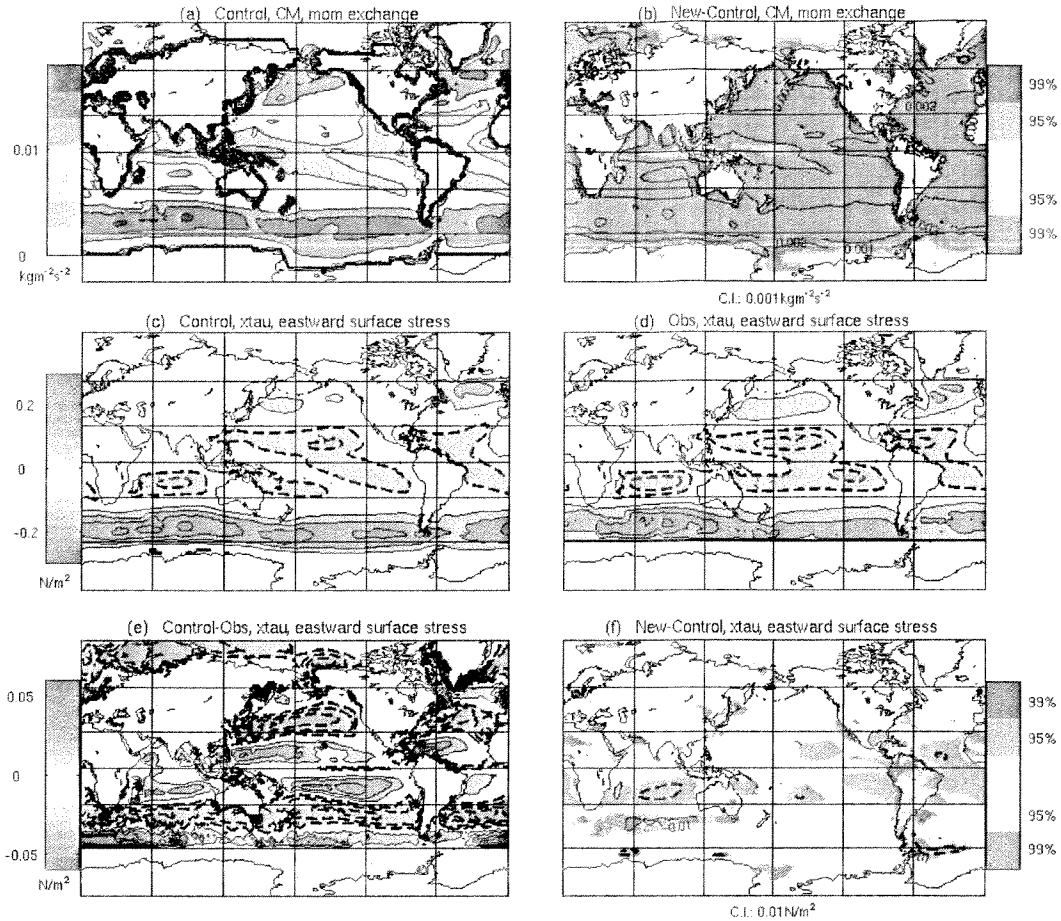

Figure 3. (a,b) Cm, drag coefficient for momentum exchange at the surface (C_m=C_D*surface wind speed) in the control run and in the new run minus the control. Contour interval is $5 \cdot 10^{-3} kgm^{-2}s^{-2}$ for (a) and $10^{-3} kgm^{-2}s^{-2}$ for (b). (c-f) Eastward surface stress at the surface in the control run (c), observations (d), control-observations (e), and new-control (f). Contour interval is $5 \cdot 10^{-2} Nm^{-2}$ for (c) and (d) and $10^{-2} Nm^{-2}$ for (e) and (f). Regions with anomalies whose statistical significance exceeds 95% are in color in (b) and (f). The zero contour is omitted and negative contours are dashed.

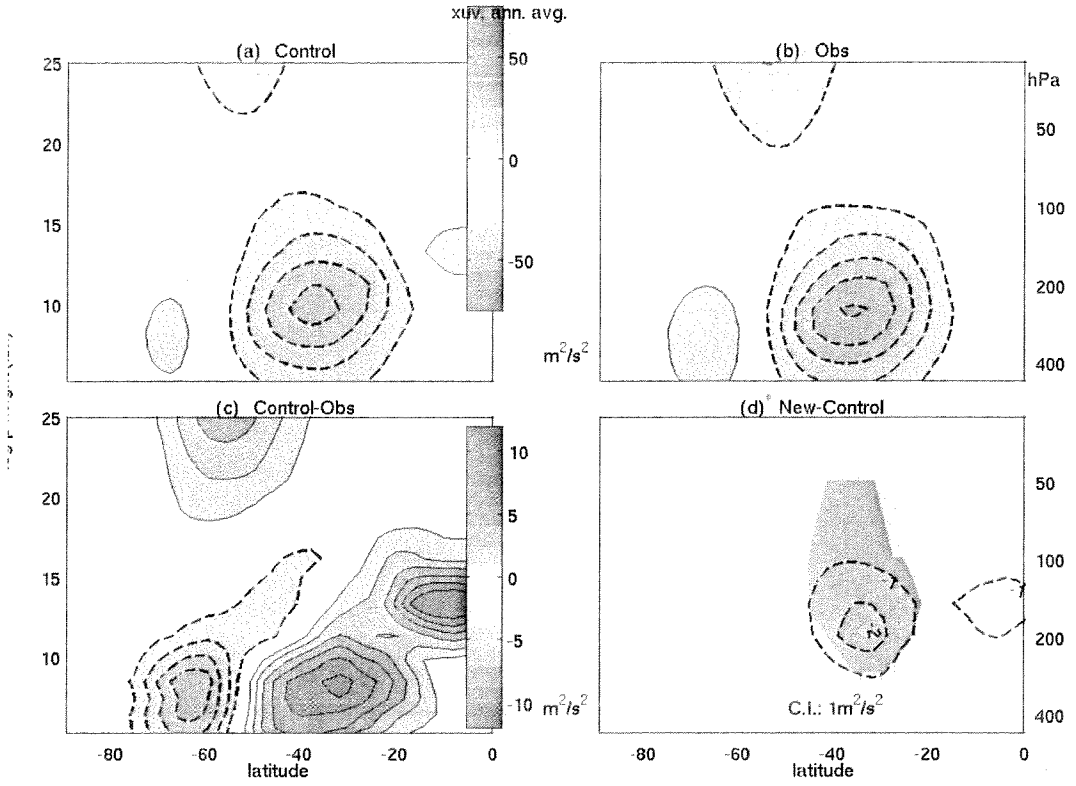

Figure 4. Momentum flux ($\overline{u'v'}$) latitude-height cross section. Contour interval is $12.5m^2s^{-2}$ for (a) and (b), $2m^2s^{-2}$ for (c), and $1m^2s^{-2}$ for (d). The zero contour is omitted and negative contours are dashed. Regions with anomalies whose statistical significance exceeds 95% (95%) are in light(dark) blue in (d).

(a) Momentum exchange over oceans in different GCMs.

Modeling Group	source	description
CAM2	Kiehl et al. [1998]	based on Large et al. [1994]
CAM5	p.181 of Neale and et al. [2010]	Large et al. [1994]
GEOS-5 (old)	Helfand and Schubert [1995]	Large and Pond [1981]
AM2.0	model development team [2004]	Beljaars [1995], $\alpha_{Charnok} = 0.018$
WRF(MM5)	page 72 of Skamarock et al. [2008]	based on Charnock [1955]
uncoupled ECMWF	page 38 of for Medium-Range Weather Forecasts [2010]	based on Charnock [1955], $\alpha_{Charnok} = 0.018$

(b) Coefficients for MOST Scheme equation relating u* to z_0 ($z_0 = \frac{A_1}{u*} + A_2 + A_3 u* + A_4 u*^2 + A_5 u*^3$)

		A_1	A_2	A_3	A_4	A_5
control	u*<0.0632456	$0.2030325E-5$	0	0	0	0
	0.0632456<u*<0.381844	-0.402451E-08	0.239597E-04	0.117484E-03	0.191918E-03	0.395649E-04
	0.381844<u*	-0.237910E-04	0.228221E-03	-0.860810E-03	0.176543E-02	0.784260E-04
new	u*<0.0632456	$0.2030325E-5$	0	0	0	0
	0.0632456<u*	-1.102451E-08	0.1593E-04	0.1E-03	2.918E-03	0.695649E-04

Table 1. The Community Atmosphere Model (CAM) has not upgraded its scheme since version 2.0 (Kiehl et al. [1998] versus section 4.11.2 of Neale and et al. [2010]).